Journal of Physiology (1993), **472**, *pp.* 177–202
With 12 figures
Printed in Great Britain

ACTIVATION OF INTERNODAL POTASSIUM CONDUCTANCE IN RAT MYELINATED AXONS

BY GAVRIEL DAVID, JOHN N. BARRETT AND ELLEN F. BARRETT

From the Department of Physiology and Biophysics, University of Miami School of Medicine, PO Box 016430, Miami, FL 33101, USA

(*Received 20 October 1992*)

SUMMARY

1. Voltage changes associated with currents crossing the internodal axolemma were monitored using a microelectrode inserted into the myelin sheath (peri-internodal region) of rat phrenic nerve fibres. This microelectrode was also used to change the potential and the ionic environment in the peri-internodal region.

2. Following stimulation of the proximal nerve trunk, the peri-internodal electrode recorded a positive-going action potential whose amplitude increased (up to 75 mV) with increasing depth of microelectrode penetration into the myelin. The resting potential recorded by the peri-internodal electrode remained within 4 mV of bath ground.

3. Confocal imaging of fibres injected peri-internodally with the fluorescent dye Lucifer Yellow revealed a staining pattern consistent with spread of dye throughout the myelin sheath of the injected internode.

4. After ionophoresis of K^+ (but not Na^+) into the peri-internodal region, the action potential was followed by a prolonged negative potential (PNP) lasting hundreds of milliseconds to several seconds. The duration of the PNP increased as the frequency of stimulation decreased. PNPs could also be evoked by sub-threshold depolarization of the internodal axolemma with peri-internodally applied current pulses. In the absence of action potentials or applied depolarization PNPs sometimes appeared spontaneously.

5. Peri-internodal application of Rb^+ also produced evoked and spontaneous PNPs. These PNPs had longer durations (up to 20 s) than those recorded from K^+-loaded internodes.

6. Spontaneous action potentials sometimes appeared during the onset of the PNP, suggesting that PNPs are associated with depolarization of the underlying axon.

7. Passage of current pulses during the PNP demonstrated that the PNP is associated with an increased conductance of the pathway linking the peri-internodal recording site to the bath. At least part of this conductance increase occurs across the internodal axolemma, since peri-internodally recorded action potentials evoked during the PNP had larger amplitudes than those evoked before or after the PNP.

8. PNPs were suppressed by tetraethylammonium (TEA, 10–20 mM) and by 4-aminopyridine (1 mM).

MS 1853

9. These results suggest that the PNPs recorded in K^+- or Rb^+-loaded myelin sheaths are produced by a regenerative K^+ or Rb^+ current that enters the internodal axolemma via K^+ channels opened by action potentials or subthreshold depolarizations.

10. When normal extracellular [K^+] was preserved (by using Na^+ rather than K^+ salts in the peri-internodal electrode), action potentials recorded within the myelin sheath were instead followed by a brief, positive after-potential that was inhibited by TEA. This finding suggests that action potentials can also activate internodal K^+ channels under normal ionic conditions.

INTRODUCTION

Myelinated axons contain depolarization-activated K^+ channels in nodal, paranodal and central internodal regions of the axolemma. Under voltage clamp, nodal K^+ channels (where present) are manifested as a depolarization-activated outward current that is sensitive to the transmembrane K^+ concentration gradient and to K^+ channel blocking agents such as TEA and/or 4-aminopyridine (4-AP) (Hille, 1967; Black, Kocsis & Waxman, 1990; reviewed in Hille, 1992). Under current clamp, nodal K^+ channels are often hypothesized if action potential duration is prolonged by TEA, 4-AP or gallamine (frog: Schmidt & Stämpfli, 1966; frog and rat: Smith & Schauf, 1981; lizard: Barrett, Morita & Scappaticci, 1988). Nodal membranes of adult mammalian myelinated axons contain fewer depolarization-activated K^+ channels than the nodal membranes of amphibian and reptilian myelinated axons (permeability ratios for peak currents $P_K/P_{Na} = 0{\cdot}06$–$0{\cdot}09$ in rat (Brismar, Hildebrand & Berglund, 1987); 0·27 in toad (Frankenhaeuser, 1959, 1962); 0·35 in lizard (Angaut-Petit, Benoit & Mallart, 1989)).

K^+ channels in paranodal and central internodal axolemmae have been studied in axons subjected to a variety of demyelinating treatments (paranode: rabbit, Chiu & Ritchie, 1980, 1981; rat and frog, Roper & Schwarz, 1989; internode: frog, Chiu & Ritchie, 1982; Grissmer, 1986; bullfrog, Chiu, Shrager & Ritchie, 1985; rabbit, Chiu & Schwarz, 1987). Some axonal delayed rectifier K^+ channels activate near the resting potential (Dubois, 1981), and it has been hypothesized that internodal K^+ channels stabilize the resting potential and help prevent re-excitation of the node during the post-discharge superexcitable period (Chiu & Ritchie, 1981, 1984; Chiu, 1982). Delayed rectifier K^+ channels in para- and internodal axolemmae also contribute importantly to the block of conduction observed when axons are demyelinated (Bostock, Sherratt & Sears, 1978). However, since in intact axons these axolemmal regions are normally covered by the myelin sheath, they experience less depolarization than the nodal axolemma during axonal activity.

Thus one might question whether, during normal activity in myelinated axons, these internodal K^+ channels experience enough change in transmembrane potential to alter their activation. Barrett & Barrett (1982) presented evidence that in myelinated frog and lizard motor axons the internodal axolemma is indeed depolarized following each action potential, to an extent approximated by the peak amplitude of the depolarizing after-potential, and David, Barrett & Barrett (1992) showed that this depolarization is sufficient to activate internodal K^+ channels. However, in mammalian myelinated axons depolarizing after-potentials

are not always detected (Kocsis & Waxman, 1981), and when detected, they are smaller and briefer than those recorded in frog and lizard myelinated axons (Gasser & Grundfest, 1936; Barrett & Barrett, 1982; Blight & Someya, 1985). None the less, analysis of electrotonic potentials and after-potentials indicates that K^+ channels do vary their opening in response to activity in mammalian myelinated axons, and suggests that at least some of these functional K^+ channels are present in paranodal and/or internodal axolemmae (Baker, Bostock, Grafe & Martius, 1987; Eng, Gordon, Kocsis & Waxman, 1988; see also Chiu, 1991).

The experiments described here investigated whether internodal axolemmal delayed rectifier K^+ channels are indeed activated following action potentials in myelinated motor axons of the rat phrenic nerve. The experiments used a microelectrode to load the myelin sheath surrounding one internode with K^+, reversing the electrochemical gradient for K^+ across the internodal axolemma, so that activation of paranodal or internodal K^+ channels could trigger a regenerative potential. We demonstrate that such regenerative K^+ potentials, termed prolonged negative potentials (PNPs), can be recorded in the myelin sheath after action potentials in rat axons. We show that these PNPs are inhibited by both TEA and 4-AP, and that Rb^+ can substitute for K^+ in promoting PNPs. Comparison of the electrical behaviour of rat and lizard motor axons suggests that rat internodal K^+ channels may be more open at rest than those in lizard axons. A possible relationship between the PNP and other bistable states reported in myelinated axons by Tasaki (1959) and Bostock, Baker & Reid (1991) is discussed.

METHODS

Preparations and solutions

Intra-axonal and peri-internodal recordings were obtained from myelinated axons innervating the diaphragm of adult (3–5 month) Sprague–Dawley rats. Animals were killed with ether, and the diaphragm was dissected with a 0·5–1·0 cm length of the phrenic nerve. A 2–5 mm length of the main intramuscular nerve bundle was then exposed by cutting the muscle fibres overlying the nerve, to enable visualization of individual myelinated fibres. Preparations were pinned to the bottom of a Sylgard-coated chamber and perfused with a physiological solution (mM: 118 NaCl, 3 KCl, 1·5 $CaCl_2$, 25 $NaHCO_3$, 1 $MgCl_2$, 10 glucose), saturated with a 95%/5% O_2/CO_2 mixture. Bath pH was maintained at 7·2–7·5, monitored with the indicator dye Phenol Red. Bath perfusion was maintained with a peristaltic pump (Gilson, Villiers Le Bel, France).

A sample of myelinated fibres in this preparation, visualized with an inverted microscope (Nikon, Japan) equipped with a 100× objective, had an average external diameter of $7·6 \pm 1·1$ μm (mean ± S.D., range 4·3–11·0 μm, $n = 104$). They retained an intact peri-neurial sheath, and did not display the characteristic signs of damage often seen in teased axons (e.g. multiple and widened clefts of Schmidt–Lanterman, widened nodal gaps, beading and vesiculation of myelin).

Action potentials were evoked by brief (40–100 μs) suprathreshold depolarizing pulses applied to the proximal nerve trunk via a suction electrode at frequencies of 0·1–1·0 Hz. Muscle contraction in response to nerve stimulation was prevented by cutting the nerve branches proximal to the terminal region, or by adding 200 μM carbachol and/or 2 mM $MnCl_2$ to the perfusing solution. In some experiments TEA (chloride salt, 5–20 mM) or 4-AP (1 mM) were added to the buffered perfusing solution.

All reagents were purchased from Sigma Chemical Co., St Louis, MO, USA.

Recording

Nerve fibres were visualized using an upright microscope (Jena, Reichert, Austria) equipped with a 32× objective. An internodal region was impaled with a microelectrode pulled with a Brown–Flaming puller (Sutter Instrument Co., San Francisco, CA, USA) and filled with one of the

following solutions (M): 0·2–0·5 K_2SO_4, 0·2 potassium citrate, 3 KCl, 3 RbCl, 1–3 NaCl or 3 NaCl with 0·05 KCl. In some cases the Ca^{2+} buffer 1,2-bis(*O*-aminophenoxy) ethane-*N*,*N*,*N*′,*N*′-tetraacetic acid (BAPTA, 10 mM) was added to the electrode filling solution to eliminate any possible contribution of Ca^{2+} in the electrode to the recorded signals. Electrode resistances ranged from 70 to 200 MΩ. Electrodes for TEA ionophoresis were filled with 1 M TEA-Cl.

Peri-internodal recordings were obtained either by gradually advancing the microelectrode into the myelin sheath (as in Fig. 1), or by withdrawing the microelectrode from an impaled axon (as in Fig. 2). A piezoelectric device was sometimes used to 'tap' the microelectrode into the myelin sheath or the axon. The term peri-internodal is meant to indicate that the electrode tip was within or beneath the myelin sheath surrounding an internode. The peri-internodal electrode thus records potential changes across the region of myelin sheath between the electrode tip and the bath, and the recorded potential will be influenced by both capacitative and resistive currents crossing the internodal axolemma. As also seen in lizard motor axons (David *et al.* 1992), peri-internodal recordings had resting potentials within 4 mV of bath ground, and displayed a positive spike when stimulation of the proximal nerve trunk evoked an action potential in the underlying axon. This peri-internodally recorded spike is produced primarily by currents crossing the large capacitance of the internodal axolemma. All peri-internodal recordings accepted for analysis had a spike amplitude of at least 10 mV.

Intra-axonal recordings were accepted for analysis if they had resting potentials of at least −60 mV, and an action potential amplitude of at least 60 mV. In twenty intra-axonal recordings the average resting potential was $-74{\cdot}4 \pm 3{\cdot}7$ mV (mean ± S.D.). Stable peri-internodal and intra-axonal recordings could sometimes be maintained for up to an hour, but the preparation was not stable enough to permit simultaneous recordings from more than one peri-internodal or intra-axonal microelectrode. Addition of 2 mM Mn^{2+} to the bath, or elevation of bath [Ca^{2+}] to 3 mM, improved the stability of intra-axonal recordings.

Voltage recording, current passage and monitoring were done using a preamplifier (Axoclamp 2A, Axon Instruments, Foster City, CA, USA) equipped with a bridge circuit. The capacitance neutralization was adjusted to optimize the voltage response to a square current pulse while avoiding oscillation. High-frequency signals like action potentials were attenuated, especially with the higher resistance electrodes, but slow after-potentials were faithfully recorded. Signals were displayed on a digital oscilloscope (Nicolet 3091, Madison, WI, USA), recorded on videotape via a recording adaptor (model 4000A PCM, Vetter Co., Rebersburg, PA, USA, sampling frequency 11–44 kHz) and later converted to analog form and redigitized (20–50 kHz) for computer-assisted analysis of action potentials and after-potentials. Slow changes in the resting potential were monitored using a Gould 2200S chart-recorder (Cleveland, OH, USA).

Most recordings were done at room temperature (21–25 °C), but some experiments used solutions maintained at higher temperatures (up to 33 °C) by passing the perfusion solution through a heated glass tube and by heat lamps in the recording cage. As expected, the duration (measured at half-peak amplitude) of peri-internodally and intra-axonally recorded action potentials was shorter at the higher temperatures (Q_{10} of 1·74 over the range 21–33 °C, $n = 98$), but there was no consistent effect of temperature on action potential amplitude or on the after-potentials. Averages are reported as means ± S.D.

Confocal microscopy of dye-filled myelin sheaths

To characterize further the peri-internodal recording site in this preparation, Lucifer Yellow CH, a cell-impermeant fluorescent dye, was ionophoresed into sites identified as peri-internodal by the presence of action potentials and a minimal (< 4 mV) resting potential. The ionophoretic microelectrode was filled with 10 mg/ml Lucifer Yellow CH (dipotassium salt) dissolved in 0·2 M K_2SO_4. After dye ionophoresis (−0·6 to −0·7 nA for 3–5 min) the main intramuscular nerve bundle, with its peri-neurial sheath still intact, was dissected away from the muscle and transferred to a glass coverslip in physiological solution. The nerve was covered with a second coverslip, which was sealed around its edge to prevent drying of the tissue. Dye distribution was then assessed with a confocal laser-scanning microscope (Olympus Corp., Lake Success, NY; fluorescein filter set).

RESULTS

The peri-internodal recording site

Figures 1 and 2 show spike potentials recorded in response to nerve stimulation as a microelectrode was advanced through the myelin sheath into an axon (Fig. 1*A*), or

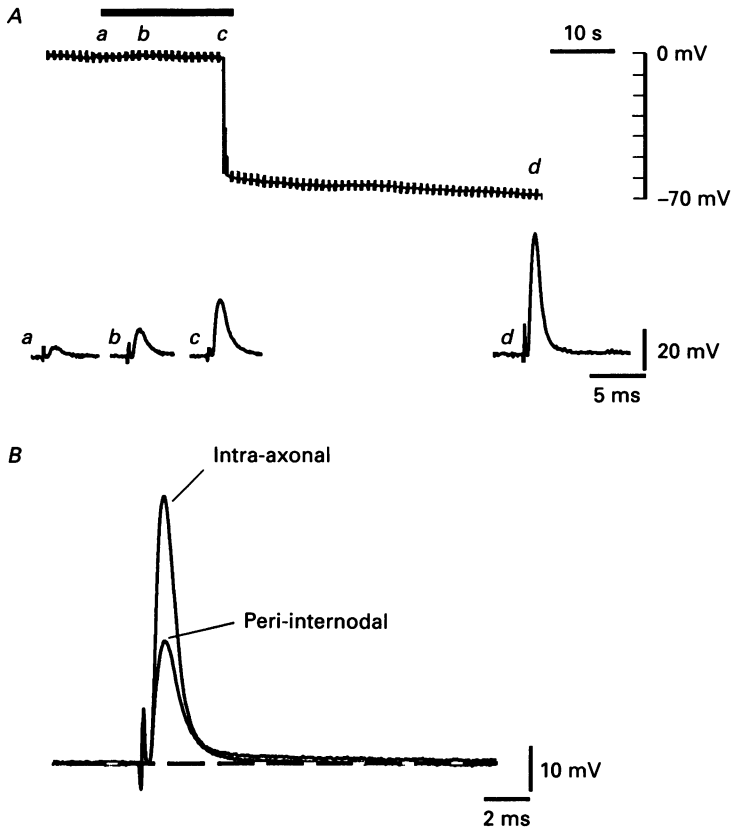

Fig. 1. *A*, voltage recordings obtained with a 0·5 M K_2SO_4-filled microelectrode, gradually inserted into the myelin sheath during suprathreshold 1 Hz stimulation of the proximal nerve trunk. The chart recorder trace (upper) displays the potential difference between the microelectrode and bath ground on a slow time scale. The thick line above the trace indicates the period of electrode advancement. Action potentials recorded peri-internodally at times *a–c* are displayed below on a fast time scale. During electrode advancement into the myelin, the amplitude of the peri-internodally recorded spike increased (*a–c*), while the resting potential remained close to 0. Further advancement of the microelectrode resulted in a potential shift to ~ -70 mV, indicating impalement of the axon (trace *d*). *B*, comparison of the intra-axonally recorded action potential with the largest peri-internodally recorded action potential from the experiment shown in *A*. The intra-axonal record had the longer depolarizing (positive) after-potential. Each trace is the average of 8 trials. In this and subsequent figures the dashed line indicates the baseline. The bathing solution contained 2 mM Mn^{2+} and 200 μM carbachol; temperature, 24 °C.

withdrawn from an axon and then from the myelin sheath (Fig. 2*A*). The intra-axonal recordings showed a large negative resting potential, and the action potential was followed by a small depolarizing after-potential (Figs 1*B* and 2*B*). The peri-

internodal recordings had a resting potential that remained within 4 mV of the bath ground, and a spike amplitude that increased as the electrode penetrated deeper into the myelin sheath (Fig. 1*A*, traces *a–c*), and decreased as the electrode was retracted from the sheath (Fig. 2*A*, traces *b–f*). This finding confirms the hypothesis of David

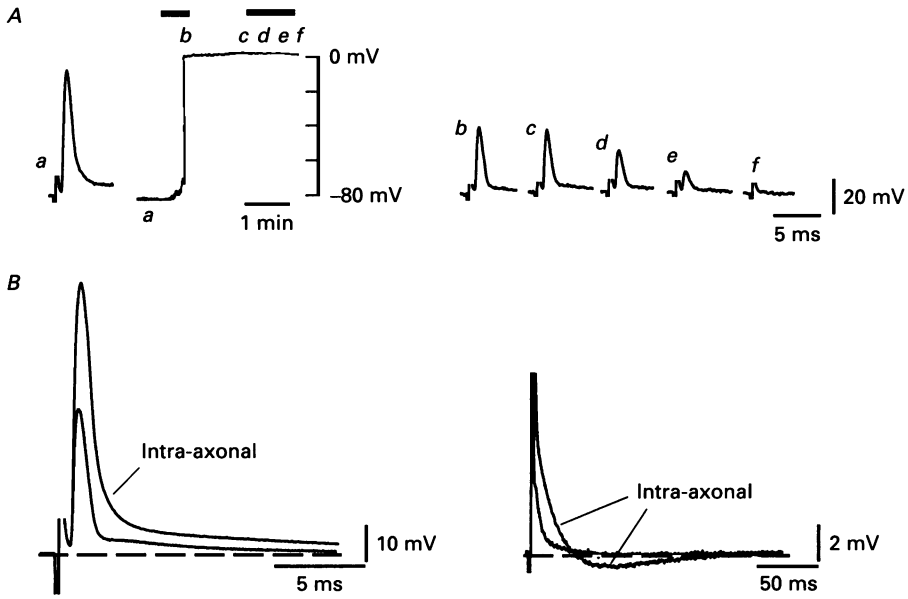

Fig. 2. Voltage recordings obtained with a microelectrode containing 3 M NaCl and 50 mM KCl as the electrode was gradually withdrawn from an axon and myelin sheath. *A*, at time *a* on the slow chart recorder trace the electrode was in an axon with a resting potential of ~ -80 mV; the intra-axonal action potential is illustrated in fast trace *a* at left. When the microelectrode was withdrawn from the axon, the resting potential changed to ~ 0 mV and the amplitude of the peri-internodal action potential decreased as the microelectrode was gradually withdrawn from the myelin sheath (fast traces *b–f* at right). The thick lines above the chart recorder trace indicate the period of electrode withdrawal. The calibrations for traces *b–f* apply also to leftmost trace *a*. *B*, superimposed action potentials (fast traces at left) and after-potentials (slow traces at right) recorded intra-axonally and peri-internodally from the axon in *A*. Each trace is the average of 50 trials. The bathing solution contained 2 mM Mn^{2+} and 200 μM carbachol; temperature, 22 °C.

et al. (1992) that the depth of electrode penetration into the myelin sheath is a major determinant of the amplitude of the peri-internodally recorded action potential.

In a sample of eighty-nine representative impalements, the largest peri-internodal spike potentials recorded in a particular internode had an amplitude that ranged from 10 (the minimal amplitude accepted for analysis) to 75 mV, with a mean amplitude of $39{\cdot}8 \pm 11{\cdot}6$ mV (S.D.) and a mean duration (at half-peak amplitude) of $0{\cdot}93 \pm 0{\cdot}26$ ms. Peri-internodally and intra-axonally recorded action potentials were compared in nine axons (mean intra-axonal resting potential $-67{\cdot}2 \pm 5{\cdot}1$ mV) in which both types of recording were obtained sequentially from the same axon. As shown by the superimposed records in Figs 1*B* and 2*B* (left), the intra-axonally

recorded action potential was larger than the peri-internodally recorded action potential. In this sample the mean action potential amplitudes were $72{\cdot}8 \pm 10{\cdot}3$ mV intra-axonally and $40{\cdot}3 \pm 17{\cdot}4$ mV peri-internodally, with a mean duration (at 50% peak amplitude) of $0{\cdot}87 \pm 0{\cdot}23$ ms intra-axonally and $0{\cdot}82 \pm 0{\cdot}21$ ms peri-internodally. As previously noted for lizard motor fibres, there was no significant correlation between the amplitudes of intra-axonal and peri-internodal spikes recorded from individual axons. The amplitude and duration of the peri-internodally recorded spike were not significantly correlated, did not vary significantly with the various electrode filling solutions (e.g. K_2SO_4 in Fig. 1, NaCl in Fig. 2), and were not altered by the presence of Mn^{2+} in the bath or BAPTA in the electrode. However, peri-internodal recordings made using a Na^+-filled electrode appeared to deteriorate more rapidly than those made using a K^+-filled electrode.

In some cases (e.g. Fig. 1) the peri-internodally recorded spike had a time course similar to that of the intra-axonally recorded action potential, whereas in other cases (Fig. 2) the peri-internodally recorded spike had a faster time course. The spike recorded peri-internodally is due mainly to current crossing the capacitance of the internodal axolemma. However, voltage transients measured after passing current from peri-internodal electrodes indicate that the time constant at the peri-internodal recording site is longer than the duration of the action potential. Thus under ideal recording conditions, the spike recorded within the myelin sheath would be expected to have a time course very similar to that of the intra-axonally recorded action potential. Leakage of current around the recording electrode would reduce the time constant at the peri-internodal recording site, and thus increase the degree to which the peri-internodally recorded spike leads the intra-axonally recorded action potential.

With an electrode filled with 1–3 M NaCl (and $\leqslant 50$ mM KCl) the peri-internodal action potential was followed by a positive after-potential whose duration was shorter than that following the intra-axonally recorded action potential (Fig. 2*B*, left; see also Fig. 11*A*). The right trace in Fig. 2*B* shows axonal after-potentials on a slower time sweep. The depolarizing–hyperpolarizing sequence of the intra-axonally recorded after-potential is similar to that described in previous studies of rat peripheral axons using K^+-filled microelectrodes (Baker *et al.* 1987). All recordings in subsequent figures were peri-internodal.

The data of Figs 1 and 2 indicate that the peri-internodal recording site is isolated from the bath by a resistance that permits the recording of action potentials, and is outside the axon because there is no resting potential. To characterize this recording site further, we ionophoresed Lucifer Yellow CH from a peri-internodal microelectrode. Figure 3 shows digitally superimposed bright field and confocal fluorescent micrographs demonstrating that staining was confined to the injected internode (Fig. 3*A*, $n = 2$). Both paranodal specializations were clearly outlined, and the enlarged image in Fig. 3*B* demonstrates that dye was concentrated in a ~ 2 μm sheath around the axon. Staining was fairly uniform in width and intensity along the internode, with no major increase at paranodes, and no sign of a peri-nuclear region. This staining pattern gives further evidence that the peri-internodal microelectrode tip was not inside the axon. The staining pattern also differs from that seen in studies where microelectrodes injected dye into the perinuclear Schwann cell cytoplasm (Konishi, 1990), or where dye (fura-2) entered the Schwann cell cytoplasm by diffusion of its acetoxymethyl ester from the bath (Jahromi, Robitaille & Charlton, 1992); in these studies dye was seen mainly in perinuclear and paranodal regions with

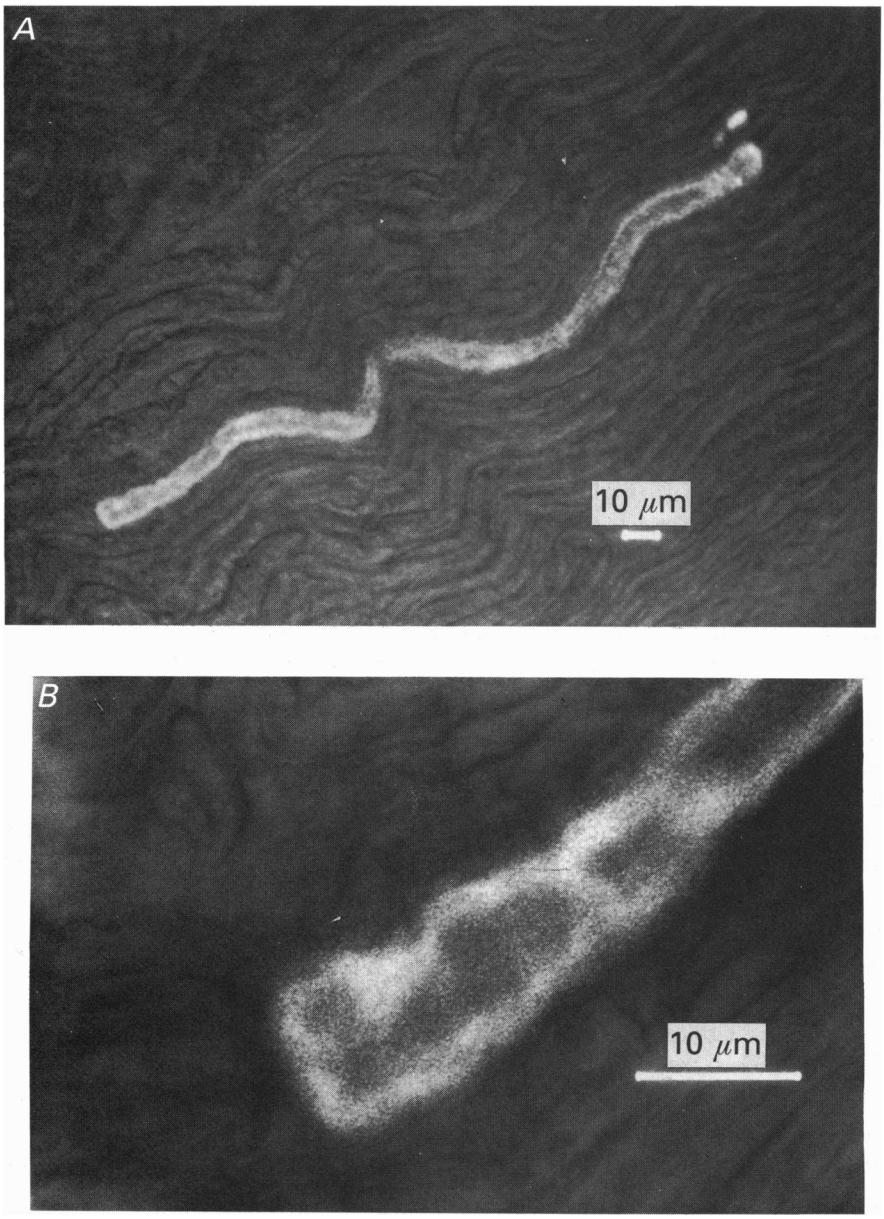

Fig. 3. Digitally superimposed confocal fluorescent and bright field images of the rat phrenic nerve following peri-internodal ionophoresis of the fluorescent dye Lucifer Yellow CH. *A*, dye penetration throughout the myelin sheath of the injected internode. The lengths of this and another nearby injected internode (not shown) were 204 and 220 μm, respectively. Fluorescent images obtained at a different focal plane demonstrated that the dark region near the centre of the illustrated internode was due to a bend in the axon rather than to a discontinuity in dye distribution. The injection site was near the right paranode. The bright dots above the injected internode indicate an unsuccessful attempt to inject an adjacent myelin sheath. *B*, higher magnification image of the left paranodal region of the internode shown in *A*, illustrating that dye was confined to the sheath and

little staining in the compact myelin. Also, electrodes inside cultured mammalian Schwann cells record a resting potential averaging −41 mV (Hoppe, Lux, Schachner & Kettenman, 1989), whereas our peri-internodal electrodes detected no significant resting potential.

These electrophysiological and morphological data thus suggest that the tip of the peri-internodal electrode was in contact with a compartment that extends throughout the length and width of the myelin sheath, but is isolated by diffusion barriers from the axoplasm, perinuclear Schwann cell cytoplasm and bath. Our morphological resolution was insufficient to determine whether the ionophoresed dye distributed within extracellular compartments (intraperiod line and/or peri-axonal space) and/or within a subcompartment of the Schwann cell intracellular space.

K^+ ionophoresis into the peri-internodal region produces both evoked and spontaneous prolonged negative potentials (PNPs)

As illustrated in Fig. 4*A*, passage of positive current (+0·1 to +0·4 nA) through a peri-internodal electrode containing a K^+ salt (sulphate, chloride or citrate) resulted in the appearance of a PNP following the stimulus-evoked action potential. These PNPs developed within 2–20 s of the beginning of K^+ ionophoresis, and could be evoked for 2–30 s after the ionophoretic current was stopped. The onset of the PNP was continuous with the falling phase of the action potential. After the peak, there was a period of slow decline followed by a rapid return to the initial potential (near 0 mV). At 1 Hz only a fraction of the action potentials were followed by a PNP in this axon, whereas at 0·2 Hz all action potentials evoked PNPs. PNP duration increased as stimulus frequency was reduced (compare traces *d* and *e* in Fig. 4*A*). In a sample of thirty-nine different peri-internodal recording sites stimulated at 1 Hz, the average PNP amplitude was $9{\cdot}4 \pm 3{\cdot}8$ mV and the average duration was 359 ± 434 ms. In a sample of eight sites stimulated at 0·2 Hz the average amplitude was $19{\cdot}1 \pm 4{\cdot}6$ mV, and the average duration was 1375 ± 845 ms. Additional PNPs could not be evoked during an on-going PNP (see Fig. 8).

Figure 4*B*, *C* shows that PNPs were also observed in the absence of nerve stimulation (see also Figs 6*Ac* and 8*Ab*). These spontaneous PNPs were preceded by a small, gradual, negative-going change in the peri-internodally recorded potential, and often produced slow (hundreds of milliseconds to seconds) oscillations in the peri-internodal potential (Fig. 4*C*). The amplitude and duration of spontaneous PNPs were similar to those of PNPs evoked by stimulating the nerve at the same frequency. Peri-internodal electrodes filled with the highest K^+ concentration (3 M) often yielded both evoked and spontaneous PNPs even when no positive current was passed through the electrode (Figs 7 and 8), probably due to K^+ leakage from the electrode tip.

Figure 4*D* demonstrates that action potentials failed to evoke PNPs when the peri-internodal electrode contained NaCl (1–3 M) instead of a K^+ salt. Thus PNP generation specifically required elevated peri-internodal [K^+], and was not simply a

---

did not enter the underlying axon. These photographs were taken within an hour after dye ionophoresis, but the staining pattern remained stable for many hours if dye bleaching was avoided. Calibration bar indicates 10 μm in both *A* and *B*.

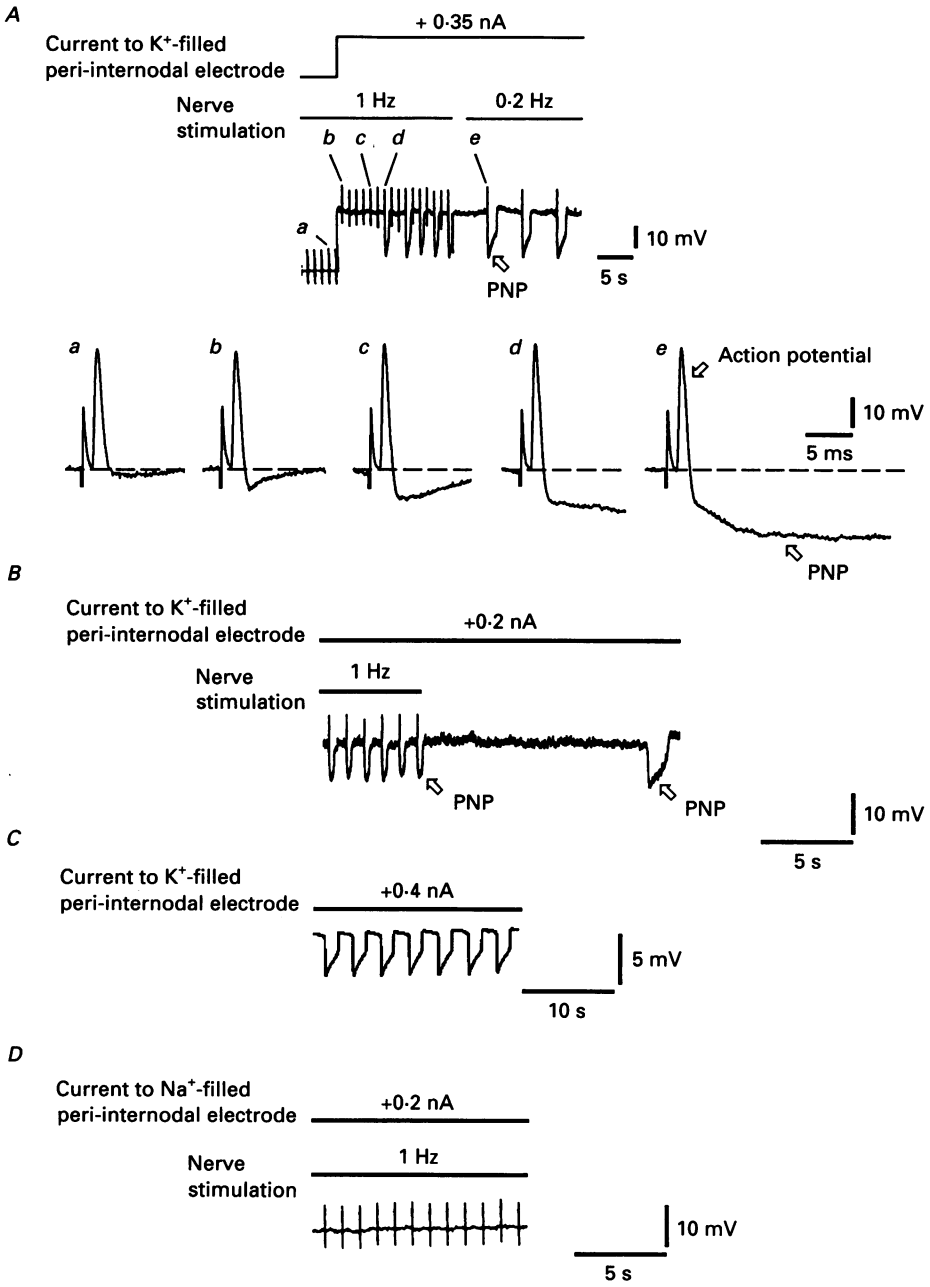

Fig. 4. *A*, *B* and *C*, prolonged negative potential (PNP) evoked following K^+ ionophoresis into the peri-internodal region. *A*, peri-internodal recordings with a 0·5 M K_2SO_4-filled microelectrode are displayed on slow (upper voltage trace) and fast (lower voltage traces) time scales before (*a*) and during (*b–e*) passage of a +0·35 nA current through the recording electrode. The times of nerve stimulation and current passage are displayed above the slow voltage trace. K^+ ionophoresis resulted in the gradual development of a PNP following the action potential (*b–d*). At a stimulation rate of 1 Hz, only a fraction of the action potentials were followed by a PNP. When the stimulation rate was decreased to 0·2 Hz, each action potential was followed by a PNP, and the duration of the PNP

consequence of passing positive current through the peri-internodal recording electrode.

Figure 5 shows that PNPs could also be evoked by applying a brief negative current pulse to a K^+-loaded peri-internodal region. Such a pulse would be expected to depolarize the underlying internodal axolemma. With a −0·3 nA pulse (traces *b*) the PNP appeared at a variable latency as an all-or-nothing phenomenon, whose amplitude matched that of the PNPs evoked at the same frequency by a larger current pulse (traces *c*) or by an action potential (trace *e*). At a given frequency, the duration of PNPs evoked by negative peri-internodal current pulses (trace *d*) was also similar to that of PNPs evoked by action potentials (trace *f*). Traces *b* and *c* indicate that PNPs can be evoked by axonal depolarizations that are subthreshold for action potential generation.

In lizard axons David *et al.* (1992) used simultaneous intra-axonal and peri-internodal recordings to demonstrate that the peri-internodally recorded PNP was accompanied by depolarization of the underlying axon. Such simultaneous recordings were not feasible in the rat phrenic nerve preparation, but Fig. 6 presents indirect evidence that rat axons also depolarize during the PNP. Traces *b* and *c* of Fig. 6*A* show records from a K^+-loaded peri-internode that exhibited both evoked (*b*) and spontaneous (*c*) PNPs. Note in trace *c* that an action potential arose during the onset of the spontaneous PNP. Such ectopic action potentials frequently occurred during the slow oscillations in peri-internodal potential recorded during K^+ ionophoresis (Fig. 4*C*), always associated with the steep portion of the developing peri-internodal negativity. Figure 6*B* shows that an action potential could also arise during the onset of a PNP evoked by an action potential. The occurrence of these spontaneous action potentials strongly suggests that PNP initiation is associated with depolarization of the underlying axon. No spontaneous action potentials occurred during the plateau phase of the PNP, perhaps because a maintained axonal depolarization increased the threshold for action potential generation (due e.g. to K^+ channel activation and/or Na^+ channel inactivation in axonal regions adjacent to the K^+-injected peri-internode).

If the PNP is associated with opening of cation channels in the internodal axolemma, then the conductance of the internodal axolemma should increase during the PNP. In David *et al.* (1992) this increased conductance was demonstrated by an experiment that recorded the peri-internodal voltage change produced by an intra-axonally applied current pulse. Since simultaneous intra-axonal and peri-internodal recordings were not possible in the rat preparation, we used the alternative strategies illustrated in Figs 7 and 8. The experiment of Fig. 7 was based on the prediction that

---

increased (*e*). No significant change in action potential amplitude or time course was observed during K^+ ionophoresis. PNPs disappeared ~ 2 s after the ionophoretic current was stopped (not shown). *B*, PNPs evoked at 1 Hz, followed by a spontaneous PNP. *C*, repetitive spontaneous PNPs recorded by electrode filled with 3 M KCl. Action potentials often occurred during the onset of these spontaneous PNPs. These ectopic action potentials are not easily visible at this slow time scale; Fig. 6 shows examples at a faster time scale. *D*, peri-internodal recording with an electrode containing 3 M NaCl, 1 min after beginning passage of a +0·2 nA current through the recording electrode. Action potentials evoked at 1 Hz were never followed by a PNP. *A* and *B*, 200 μM carbachol; *C*, 2 mM Mn^{2+}; *D*, 200 μM carbachol and 2 mM Mn^{2+}. Temperature, 25 °C in *A* and *B*, 23 °C in *C*, 22 °C in *D*.

if the conductance of the internodal axolemma increases during the PNP, the input conductance measured at the peri-internodal recording site should also increase. This was indeed the case, since current pulses applied from a peri-internodal electrode during a PNP (trace *b*) produced a smaller voltage response than current pulses

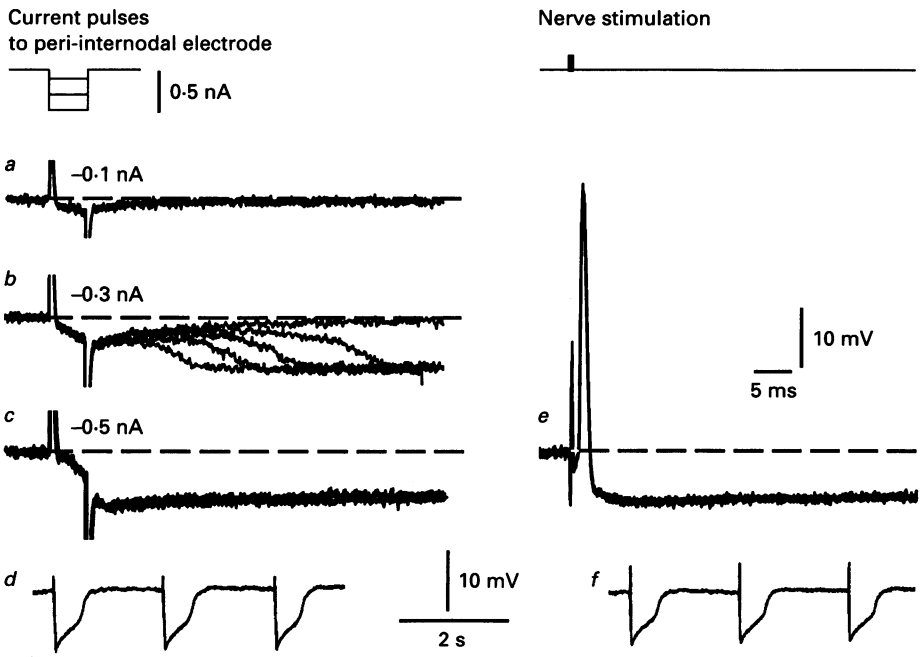

Fig. 5. PNPs evoked by applying short negative current pulses to the peri-internodal region. In *a–d* 5 ms current pulses of the indicated magnitudes were delivered at 0·5 Hz. Current pulses of −0·1 nA (*a*) did not evoke PNPs. At −0·3 nA (*b*) PNPs appeared in an all-or-nothing manner with a variable latency. At −0·5 nA (*c*) PNPs were evoked with each current pulse and were similar in amplitude and time course to PNPs evoked by suprathreshold stimulation of the proximal nerve trunk at 0·5 Hz (*e*). Slower traces *d* and *f* show the full time course of PNPs following the peri-internodal current pulse (*d*) or nerve stimulation (*f*). The microelectrode was filled with 0·2 M K_2SO_4, and K^+ ionophoresis was maintained throughout the experiment (+0·14 nA). Three signals were superimposed in *a*, and five signals were superimposed in *b*, *c* and *e*. 200 μM carbachol, 22 °C.

applied before the PNP (trace *a*, with superimposed voltage changes in trace *c*). The difference between voltage responses elicited before and during the PNP was small, but was consistently seen ($n = 3$). The direction of this difference is compatible with the hypothesis that the peri-internodal input conductance increases during the PNP. However, this result does not indicate whether the conductance increase occurs in the axolemma and/or the myelin sheath, which are connected in parallel in the pathway linking the peri-internodal recording site to the bath.

This question was resolved by comparing the amplitudes of peri-internodally recorded action potentials elicited before and during PNPs. Figure 8 shows that the peri-internodally recorded action potential was always larger during a PNP, whether the PNP arose spontaneously (*A*) or following passage of negative current from the peri-internodal electrode (*B*). Figure 8*C* shows that this was also true for peri-

internodally recorded action potentials evoked during PNPs generated by prior action potentials. Action potential amplitude remained elevated during most of the PNP (*C*). As explained below, this increase in the amplitude of the peri-internodally recorded action potential suggests that the major conductance increase during the PNP occurs across the axolemma.

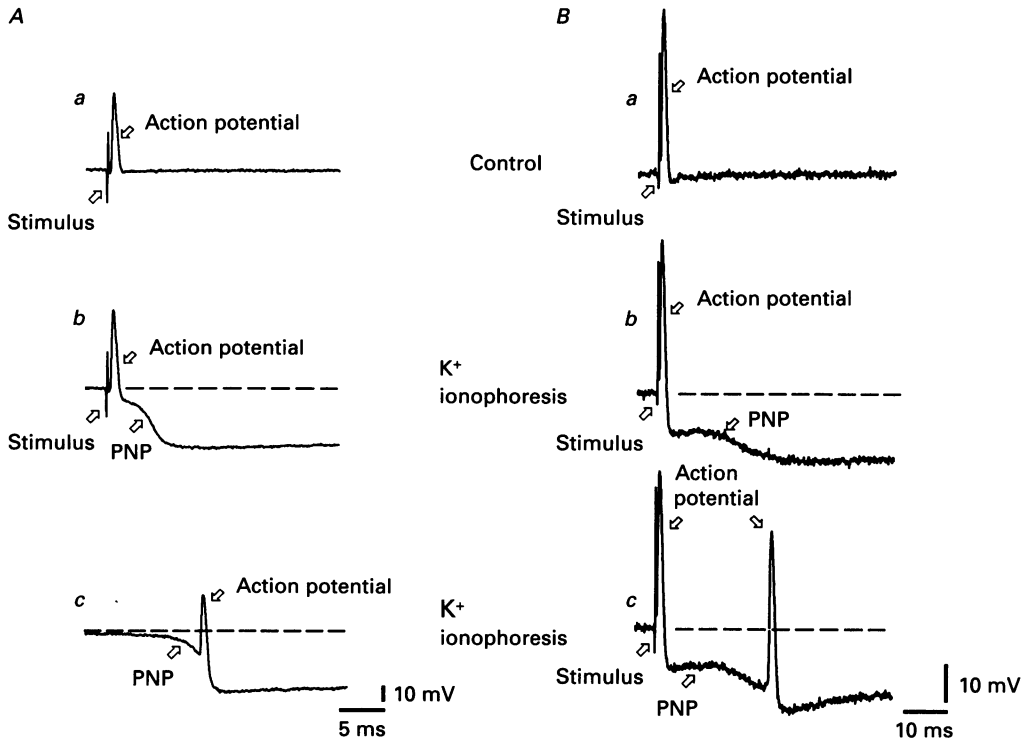

Fig. 6. Action potentials recorded during the onset of PNPs. *A*, peri-internodal recordings before (*a*) and ~ 10 s after (*b*, *c*) the onset of K^+ ionophoresis (+0·5 nA). Stimulation of the proximal nerve trunk during K^+ ionophoresis evoked an action potential followed by a PNP (*b*). When nerve stimulation was stopped, spontaneous PNPs appeared, and an action potential occurred during the rising phase of some PNPs (*c*). *B*, similar experiment, in which the PNP evoked by nerve stimulation (*b*) sometimes triggered an additional action potential (*c*). These additional action potentials suggest that the onset of the PNP is associated with depolarization of the underlying axon. Electrodes were filled with 0·2 M potassium citrate in *A* and 0·2 M K_2SO_4 in *B*. *A* and *B*, 200 μM carbachol; *A*, 3 mM Ca^{2+}; *B*, 2 mM Mn^{2+}. Temperature, 30 °C in *A*, 22 °C in *B*.

The reasoning underlying this interpretation is as follows. The peri-internodally recorded action potential has both resistive and capacitative components. The increase in the amplitude of this potential measured during the PNP is unlikely to arise from an increase in the capacitative component, because (1) there is no reason to believe that membrane capacitances changed during the PNP, and (2) the axonal action potential (which drives the capacitative component of the peri-internodally recorded signal) probably decreased rather than increased during the PNP. The reason for statement (2) is that the axon appears to depolarize during the PNP (Fig. 6), and depolarization *reduces* the amplitude of the axonal action potential (Tasaki, 1952; Woodbury, 1952). Thus the increase in the peri-internodally recorded action potential observed during the PNP was most probably due to an increase in the resistive component of this signal. The internodal

axolemma and myelin sheath are connected in series in the pathway linking the interior of the axon to the bath. Thus the resistive component of the voltage change recorded by an electrode in the internodal peri-axonal space in response to an intra-axonally applied current pulse will be proportional to the ratio $R_{my}/(R_{my}+R_{int})$, where R_{my} and R_{int} are, respectively, the resistances of the

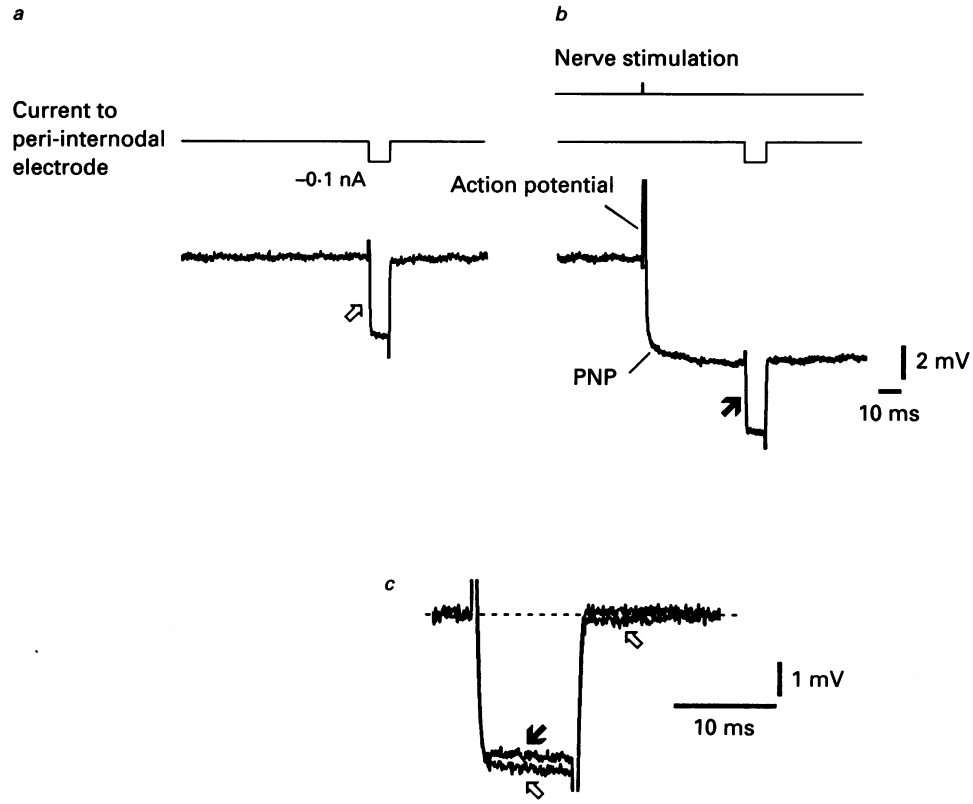

Fig. 7. Voltage responses evoked before *a*, open arrow and during *b*, filled arrow the PNP by a 10 ms current pulse (−0·1 nA) applied via the peri-internodal recording electrode. *c*, superimposed responses showing that the voltage change was smaller during the PNP, indicating a decreased input resistance at the peri-internodal recording site. A reviewer raised the possibility that the difference between the voltage signals recorded before and during the PNP might have arisen because the voltage signal before the PNP included a component due to channels activated by the pulse. However, we think that any such active component was small, because the difference between the voltage responses superimposed in *c* developed quickly and remained steady, rather than increasing over time. In this experiment (and in Fig. 8*A* and *B*) PNPs occurred even in the absence of applied ionophoretic current, probably due to K^+ leak from the 3 M KCl-filled electrodes. 2·0 mM Mn^{2+}, 24 °C.

myelin sheath and internodal axolemma. (For a peri-internodal electrode whose tip resides within rather than beneath the myelin sheath, this ratio must be modified by subtracting from R_{my} and adding to R_{int} the resistance of the myelin sheath between the electrode tip and the axolemma.) During the PNP the resistive component of the peri-internodally recorded voltage response should thus increase if R_{int} decreases, and decrease if R_{my} decreases. Using the action potential as the intra-axonally applied current pulse, the most reasonable way to explain the PNP-associated increase in the peri-internodally recorded spike (Fig. 8) is to postulate a decrease in R_{int}.

The axolemmal conductance increase associated with the PNP in rat axons must occur mainly across internodal rather than nodal axolemma, for several reasons. First, one would expect that following peri-internodal K^+ ionophoresis, $[K^+]$ would be higher outside the internodal axolemma than outside the neighbouring nodal

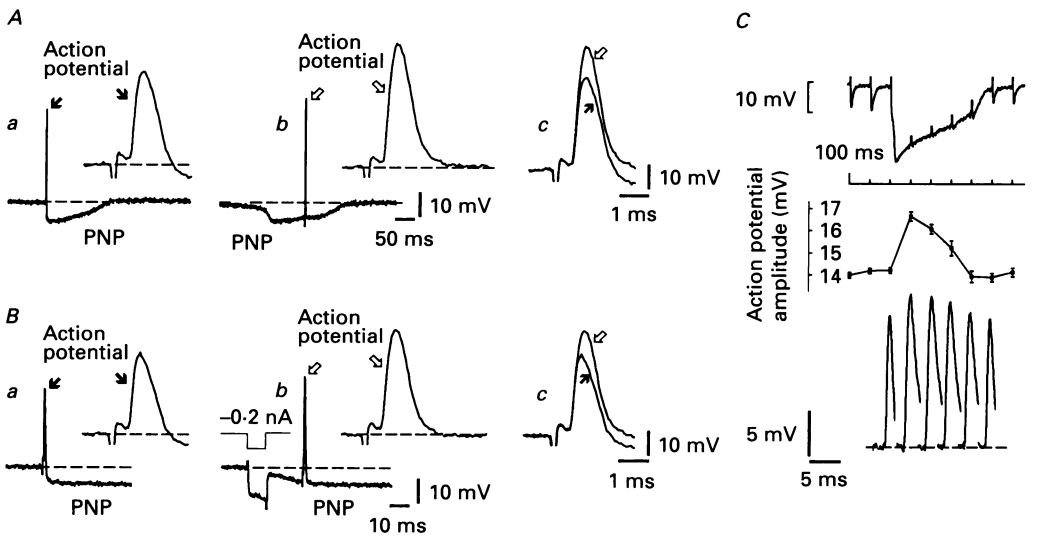

Fig. 8. Comparison of peri-internodally recorded action potentials before and during PNPs. In *A* and *B*, *a* and *b* show at slow (lower) and fast (upper) time scales the action potentials evoked by stimulation of the proximal nerve trunk before a PNP (*a*) and during a spontaneous PNP (*Ab*) or during a PNP evoked by a short negative current pulse applied to the peri-internodal region (*Bb*, as in Fig. 5). Parts *c* of *A* and *B* superimpose action potentials evoked before (filled arrow) and during (open arrow) the PNP, demonstrating the larger amplitude of action potentials evoked during the PNP. *C*, top trace shows a PNP evoked by one of a series of action potentials evoked at 10 Hz (action potential amplitudes are truncated). Bottom trace superimposes on a faster time scale the action potentials evoked before, during and after the PNP. The middle trace plots the average action potential amplitude ($n = 19$) as a function of time (same scale as in top trace), demonstrating that action potential amplitude remained elevated throughout most of the PNP. *A* and *B*, 3 M KCl electrode, no ionophoretic current; *C*, 0·5 M K_2SO_4 electrode, steady + 0·3 nA ionophoretic current. *A* and *B*, 2 mM Mn^2; *C*, 1·5 mM Mn^{2+} and 200 μM carbachol. Temperature, 24 °C in *A*, *B* and *C*.

axolemmae. Second, as mentioned earlier, mammalian nodes have relatively few K^+ channels. Finally, an inward K^+ current at the node would give rise to a peri-internodal signal opposite in polarity to the recorded PNP, and an outward K^+ current at the node could not account for the prolonged, regenerative nature of the PNP.

PNPs following Rb^+ ionophoresis

Rb^+ passes readily through axonal delayed rectifier K^+ channels (permeability ratio $P_{Rb}/P_K = 0{\cdot}76$–$0{\cdot}92$ in frog axons, Hille, 1973; Plant, 1986). Figure 9 shows that peri-internodal ionophoresis of Rb^+ could substitute for K^+ ionophoresis in supporting both evoked (*A*) and spontaneous (*B*) PNPs. A spontaneous action

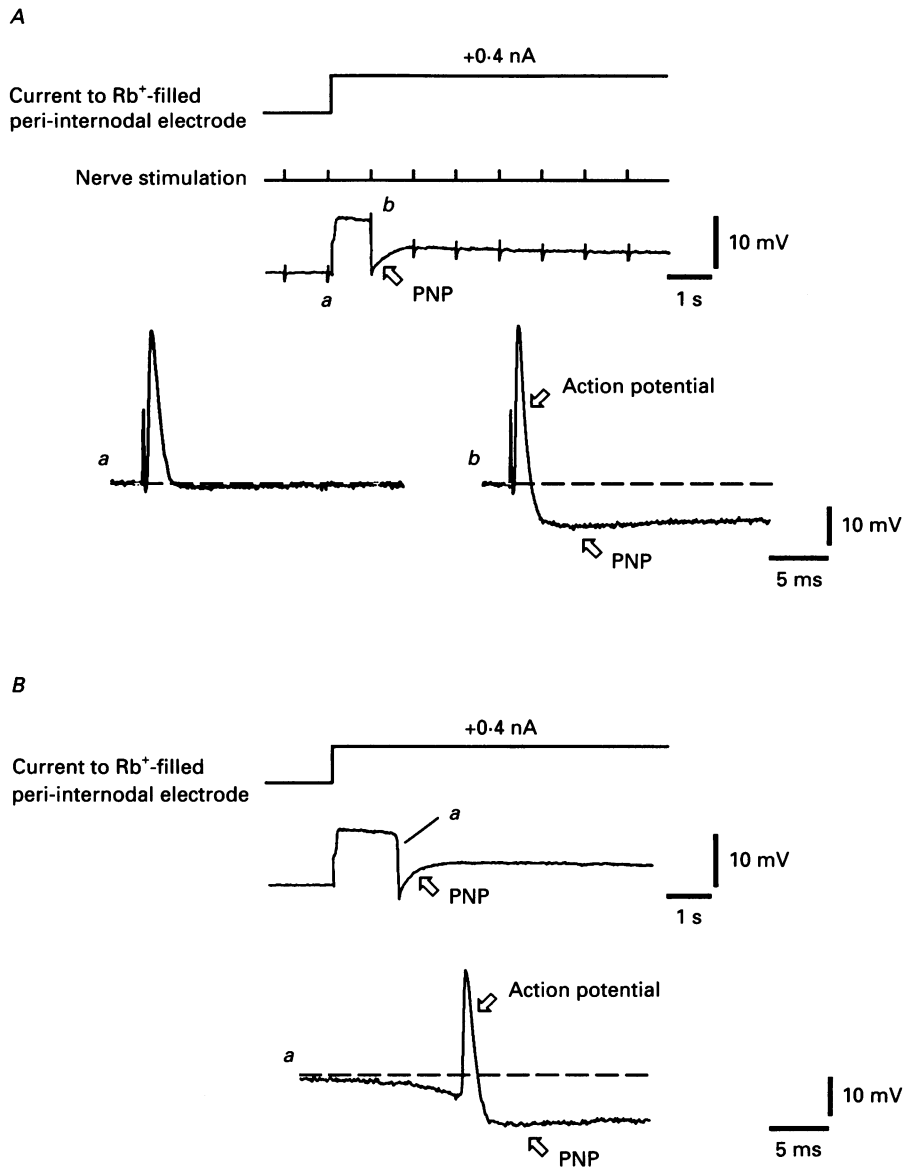

Fig. 9. Rb^+ ionophoresis into the peri-internodal region supports PNPs. *A*, slow voltage recording (upper trace) and action potentials (lower traces) evoked by nerve stimulation at 1 Hz before (*a*) and during (*b*) passage of a +0·4 nA current through a peri-internodal electrode filled with 3 M RbCl. An action potential evoked ~ 1 s after the onset of Rb^+ ionophoresis was followed by a long-lasting PNP. Action potentials evoked during this PNP did not evoke additional PNPs. *B*, slow (upper) and fast (lower) voltage traces illustrate the appearance of a spontaneous PNP ~ 1·5 s after the onset of Rb^+ ionophoresis. An action potential occurred at the onset of this spontaneous PNP (see also Fig. 6*Ac*). In both *A* and *B* the PNP continued throughout the entire period of Rb^+ ionophoresis (~ 20 s). The bathing solution contained 2 mM Mn^{2+} and 200 μM carbachol; temperature, 22 °C.

potential occurred during the onset of the spontaneous PNP, suggesting that the PNPs recorded following Rb^+ ionophoresis were also associated with axonal depolarization. Interestingly, Rb^+ PNPs lasted much longer than K^+ PNPs: in five experiments Rb^+ PNPs lasted more than 10 s, and during 1 Hz stimulation the PNP lasted 794 ± 373 ms ($n = 5$), compared to a mean duration of 359 ms for K^+ PNPs at this frequency. This PNP prolongation may be related to rubidium's ability to slow inactivation of delayed rectifier channels (Plant, 1986; see also Mueller, 1958). The mean amplitude of action potentials recorded with Rb^+-filled microelectrodes ($37{\cdot}3 \pm 14$ mV, $n = 10$) did not differ significantly from that recorded with K^+- and Na^+-filled microelectrodes.

Inhibition of the PNP by K^+ channel blockers

Figure 10*A* shows that bath application of 20 mM TEA suppressed the PNPs evoked in K^+-loaded internodes. At this concentration, TEA suppressed PNPs within 5–20 min in all seven axons tested. In three of these experiments this suppression was partially reversible within 10–20 min (Fig. 10*A*). The PNP evoked in Rb^+-loaded internodes was also suppressed by 20 mM TEA (not shown). Lower bath TEA concentrations (10 mM) required up to 60 min to block the PNP ($n = 2$), and in 5 mM TEA PNPs persisted after more than 60 min of drug exposure. The PNP was suppressed within 2–10 min following localized ionophoretic application of TEA from an electrode positioned near the K^+-injected internode (Fig. 10*B*, $n = 4$), and in the illustrated experiment this suppression was partially reversible within 3 min. The efficacy of this localized application indicates that TEA's suppression of the PNP was probably due to actions near the injected internode rather than to actions on motor terminals or remote parts of the myelinated axon.

Bath application of 1 mM 4-AP also suppressed the PNP within 5–20 min ($n = 9$), and in two of these experiments this suppression was partially reversible within 20 min (Fig. 10*C*). In two experiments 4-AP also induced spontaneous action potentials and repetitive after-discharges.

These results thus suggest that the K^+ channels involved in PNP generation are either sensitive to both TEA and 4-AP, or consist of a mixed population of TEA-sensitive and 4-AP-sensitive channels. These K^+ channels are probably not Ca^{2+} activated, since PNP generation was not inhibited by addition of 2–4 mM Mn^{2+} to the bath, or by inclusion of 10 mM BAPTA within the peri-internodal K^+-injecting electrode.

Evidence presented so far is consistent with the hypothesis that PNP generation in rat motor axons has a mechanism similar to that proposed for lizard motor axons by David *et al.* (1992), i.e. that in the presence of high peri-internodal $[K^+]$, depolarization of the underlying internodal axolemma initiates a PNP by opening axolemmal K^+ channels. Because of the reversed transmembrane electrochemical K^+ gradient, K^+ flows from the peri-internodal space into the axon, depolarizing the axon and opening more K^+ channels. This scheme thus accounts for the regenerative, all-or-none nature of the PNP (Fig. 5).

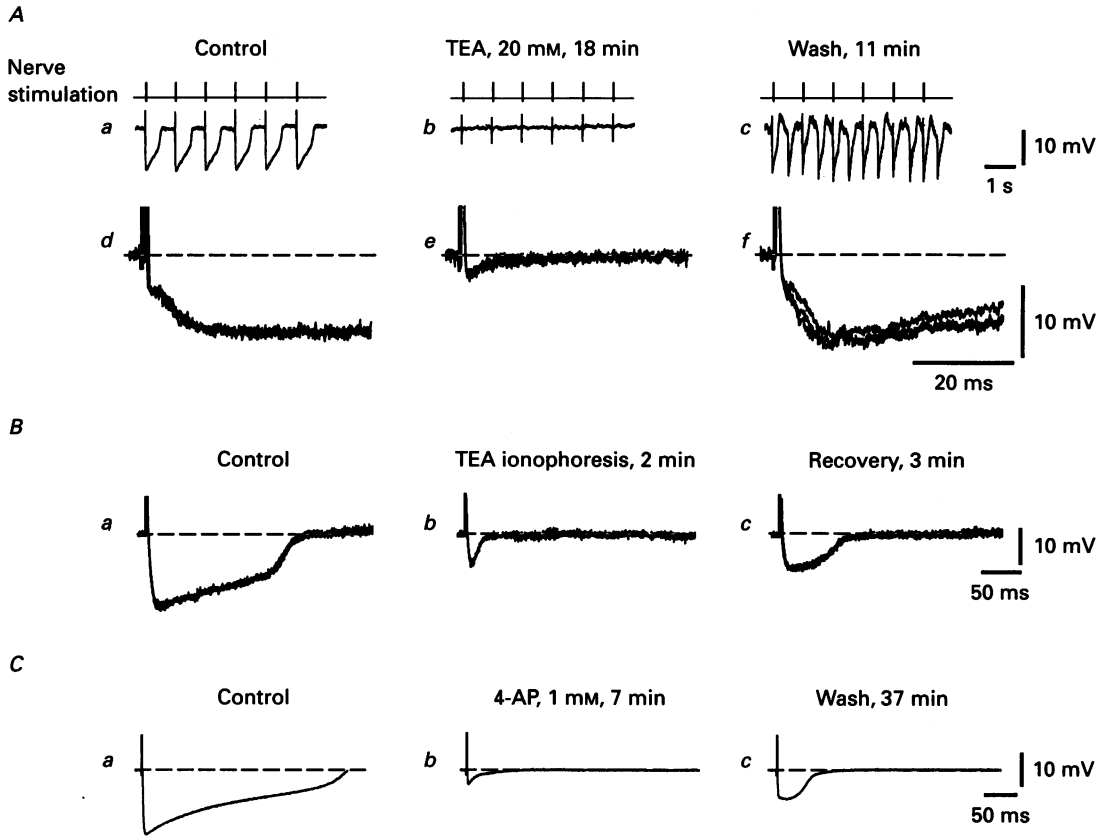

Fig. 10. K^+ channel blockers suppress the PNP. *A*, bath application of TEA. Peri-internodal recordings from a K^+-loaded internode on slow (chart recorder, *a–c*) and fast (*d–f*) time scales, before (*a* and *d*), during bath application of 20 mM TEA (*b* and *e*), and after wash-out (*c* and *f*). Both evoked and spontaneous PNPs appeared during TEA wash-out. Three superimposed traces are shown in each of *d–f*. Spike amplitudes were 48, 30 and 25 mV in control, TEA and wash, respectively. *B*, localized application of TEA. Peri-internodal recordings before (*a*), following 2 min of TEA ionophoresis (*b*) and 3 min after TEA ionophoresis was discontinued (*c*). TEA was ionophoresed from an electrode filled with 1 M TEA-Cl, positioned outside the K^+-injected internode, using 5 s, +15 nA current pulses repeated every 6 s. Three superimposed traces are shown in each of *a–c*. Spike amplitudes were 14, 14 and 12 mV during control, TEA and recovery, respectively. *C*, bath application of 4-AP. Peri-internodal recordings before (*a*), after 7 min perfusion with 1 mM 4-AP (*b*) and after 37 min wash-out of 4-AP (*c*). Action potential amplitudes were 34, 31 and 23 mV in control, 4-AP and wash, respectively. Each trace is the average of 20 responses. K^+ ionophoresis was maintained throughout the experiment by passage of +0·4 nA (*A*), +0·13 nA (*B*) or +0·2 nA (*C*) through the recording electrode (0·2 M potassium citrate in *A* and 0·2 M K_2SO_4 in *B* and *C*). *A* and B, 200 μM carbachol; *C*, 200 μM carbachol plus 2 mM Mn^{2+}. Temperature, 30 °C in *A*, 21 °C in *B* and 25 °C in *C*.

Peri-internodal recordings in normal extracellular [K^+]

In contrast, in the presence of low/normal peri-internodal [K^+], the trans-membrane electrochemical K^+ gradient would favour K^+ movement in the opposite direction, i.e. from the axon into the peri-internodal region. Opening of internodal K^+

channels during or following the action potential would thus be expected to produce a positive-going potential change in the peri-internodal space and a hyperpolarization of the internodal axolemma, thereby de-activating axolemmal delayed rectifier K^+ channels and quickly terminating the recorded potential changes. Figure 11*A* shows

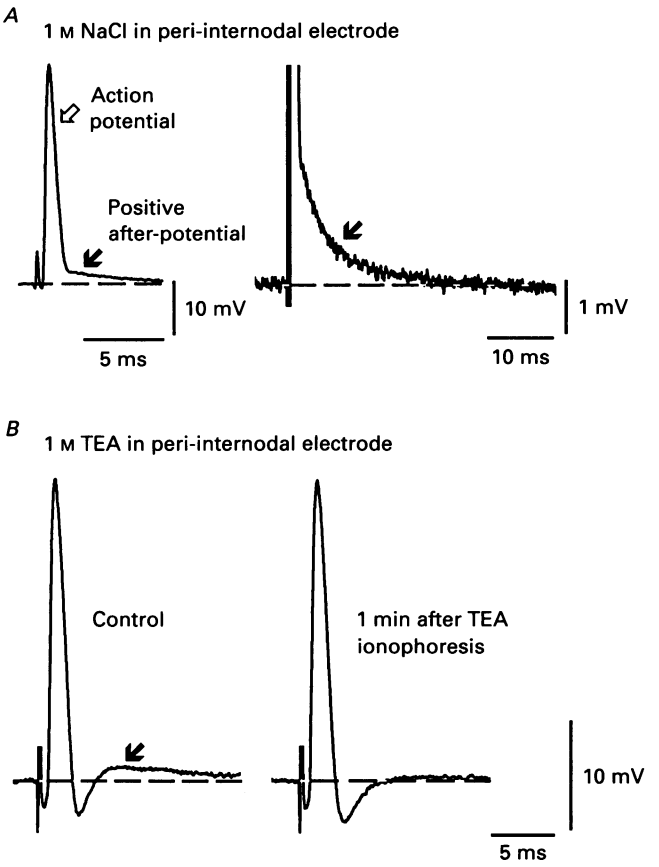

Fig. 11. Action potentials and after-potentials recorded in normal extracellular $[K^+]$, and the effect of peri-internodal application of TEA. *A*, voltage recordings from a peri-internodal electrode filled with 1 M NaCl, on fast (left) and slow (right) time scales. *B*, voltage recordings from a peri-internodal electrode filled with 1 M TEA-Cl, before (left) and after (right) a 1·0 nA, 1 min ionophoretic application of TEA from the recording electrode. TEA suppressed the positive after-potential (dark arrow), and no recovery was observed for ~ 5 min after stopping the TEA ionophoresis. *A* and *B*, 2 mM Mn^{2+} and 200 μM carbachol. Temperature, 22 °C in *A*, 23 °C in *B*.

that a brief, positive after-potential was indeed recorded with NaCl-filled peri-internodal electrodes (see also Fig. 2).

Figure 11*B* demonstrates that peri-internodal TEA ionophoresis suppressed this positive after-potential. In four such experiments TEA ionophoresis reduced the amplitude of the positive after-potential to ~ 50% of its control value within

30–60 s, with no consistent change in action potential amplitude. A similar result was seen in lizard motor axons by David *et al.* (1992). These findings suggest that action potentials can indeed activate internodal K^+ channels under physiological conditions, and that the positive after-potential recorded peri-internodally in normal extracellular $[K^+]$ is due to K^+ efflux from the axon.

In Fig. 11*B* a negative after-potential intervened between the action potential and the positive after-potential, and was enhanced following TEA ionophoresis. Similar phenomena were also seen in lizard motor axons using peri-internodal electrodes filled with physiological saline (David *et al.* 1992). We hypothesize that this negative after-potential is due to a return current produced as a consequence of the ionic currents that mediate action potential repolarization. The precise nature and localization of these repolarizing currents are not entirely clear; rat nodes have few delayed rectifier channels, so paranodal (or motor terminal) delayed rectifier channels and/or nodal leak channels may be involved. However, we cannot exclude the possibility that the negative after-potential is a recording artifact: this after-potential was not recorded consistently with 'low K' electrodes (Figs 2*B* and 11*A*), and the high-resistance microelectrode (or current leakage around it) might have distorted the amplitude and time course of fast voltage changes.

DISCUSSION

Mechanism of the prolonged negative potential (PNP) in rat axons

The experiments described here demonstrate that when K^+ is ionophoresed into the myelin sheath of a rat motor axon, brief depolarization of the underlying internodal axolemma can produce a regenerative peri-internodal potential, the PNP (Figs 4 and 5). We present evidence that this PNP is accompanied by depolarization of the underlying axon (Fig. 6) and is associated with a conductance increase (Fig. 7), and that most of this conductance increase occurs across the internodal axolemma rather than the myelin sheath or nodal axolemma (Fig. 8). This conductance increase is probably mediated by delayed rectifier K^+ channels, because PNPs could be recorded when the peri-internodal electrode contained high concentrations of K^+ or Rb^+, but not Na^+ (Figs 4 and 9). Also, PNP generation was inhibited by two K^+ channel blockers, TEA and 4-AP (Fig. 10).

The PNP recorded in rat motor axons was similar to that recorded in lizard motor axons by David *et al.* (1992), except that in lizard axons K^+-injected peri-internodes never showed spontaneous PNPs, and PNPs were not inhibited by 4-AP. A preliminary report (Kapoor, Smith, Felts & Davies, 1992) indicates that similar potentials, also inhibited by TEA and 4-AP, can be recorded in rat dorsal column and spinal root axons.

The observations that the PNP can be initiated by depolarizations subthreshold for action potential generation (Fig. 5), and is inhibited by TEA, suggest that PNP generation involves a subset of delayed rectifier K^+ channels that activate at potentials near the resting potential and are blocked by TEA (frog: Dubois, 1981; rat: Roper & Schwarz, 1989). These channels are present in nodal, paranodal and internodal axolemmae of mammalian axons (Ritchie & Chiu, 1981; Wilson & Chiu, 1990). The high concentrations of TEA required to block PNP generation (10–20 mM) are consistent with the TEA sensitivity reported for K^+ channels in internodal membranes of mammalian and amphibian axons (rat and rabbit paranodes: 30% block in 20–60 mM TEA, Chiu & Ritchie, 1980, 1981; frog internodes: 80–90% block with 10–20 mM TEA, Chiu & Ritchie, 1982; Chiu, Shrager & Ritchie, 1985; Grissmer,

1986). TEA-sensitive K^+ channels are also involved in PNP generation in lizard axons (David *et al.* 1992).

In rat axons (but not lizard axons) PNP generation was also inhibited by 1 mM 4-AP. Rat axons have many 4-AP-sensitive K^+ channels in paranodal axolemmal membranes (Roper & Schwarz, 1989). Perhaps during action potential activity these paranodal membranes depolarize sufficiently to activate some of these channels (Baker *et al.* 1987).

In K^+-loaded lizard internodes, simultaneous intra-axonal and peri-internodal recordings showed that the internodal axolemma was depolarized by at least 20–30 mV at the peak of the PNP and by at most 1–2 mV between PNPs (David *et al.* 1992). In rat axons the intra-axonal depolarization could be estimated only indirectly. The observation that action potential propagation was not blocked during PNPs suggests that the sustained depolarization was less than the 15–20 mV found to block action potential conduction in the experiments of Maruhashi & Wright (1967). Also, since spontaneous action potentials occurred only occasionally at the onset of PNPs, it is likely that the PNP-associated axonal depolarization was less than the 20–30 mV found necessary for consistent action potential initiation by Chiu, Ritchie, Rogart & Stagg (1979) and Brismar (1980).

Comparison of the PNP with other bistable states in myelinated axons

The oscillations in peri-internodal potential often recorded during steady K^+ ionophoresis (Fig. 4*C*) were most probably accompanied by shifts in the membrane potential of the underlying axon, because ectopic action potentials frequently occurred at the onset of the PNP (Fig. 6; see also Fig. 6 in David *et al.* 1992). These shifts in potential suggest similarities to the bistable states of membrane potential reported by Tasaki (1959) in toad myelinated axons and to the bimodal distribution of thresholds measured by Bostock *et al.* (1991) in human axons recovering from ischaemia. Figure 12 shows a schematic diagram of the postulated relationship between the K^+ equilibrium potential (E_K) and the axonal transmembrane potential (E_m) along the length of an axon in these three experimental situations. Note that in all three situations, there is a region of axonal membrane in which E_K is more depolarized than E_m. In Fig. 12*A*, representing the experiments reported here and in David *et al.* (1992), this region of reversed K^+ gradient is localized to a K^+-injected internode. In Fig. 12*B*, representing one of the experiments described in Tasaki (1959), this region is a single node exposed to high external [K^+]. In Fig. 12*C*, representing a post-ischaemic axon, external potassium concentration ($[K^+]_o$) is higher and intra-axonal [K^+] is lower than normal, due to K^+ loss from the axon during the ischaemic period, and E_m is hyperpolarized due to activation of the electrogenic Na^+,K^+-ATPase in the post-ischaemic period. E_K might be more depolarized for internodal than for nodal membranes during the post-ischaemic period, because of higher nodal pump activity (due to more nodal Na^+ entry and higher concentration of Na^+,K^+-ATPase at nodes: Ariyasu, Nichol & Ellisman, 1985) and because of faster diffusion of accumulated extracellular K^+ away from nodal than from internodal membranes. In all three cases, opening of K^+ channels in the axonal region(s) where E_K is more depolarized than E_m would lead to a regenerative influx of K^+. The resulting axonal depolarization would be expected to

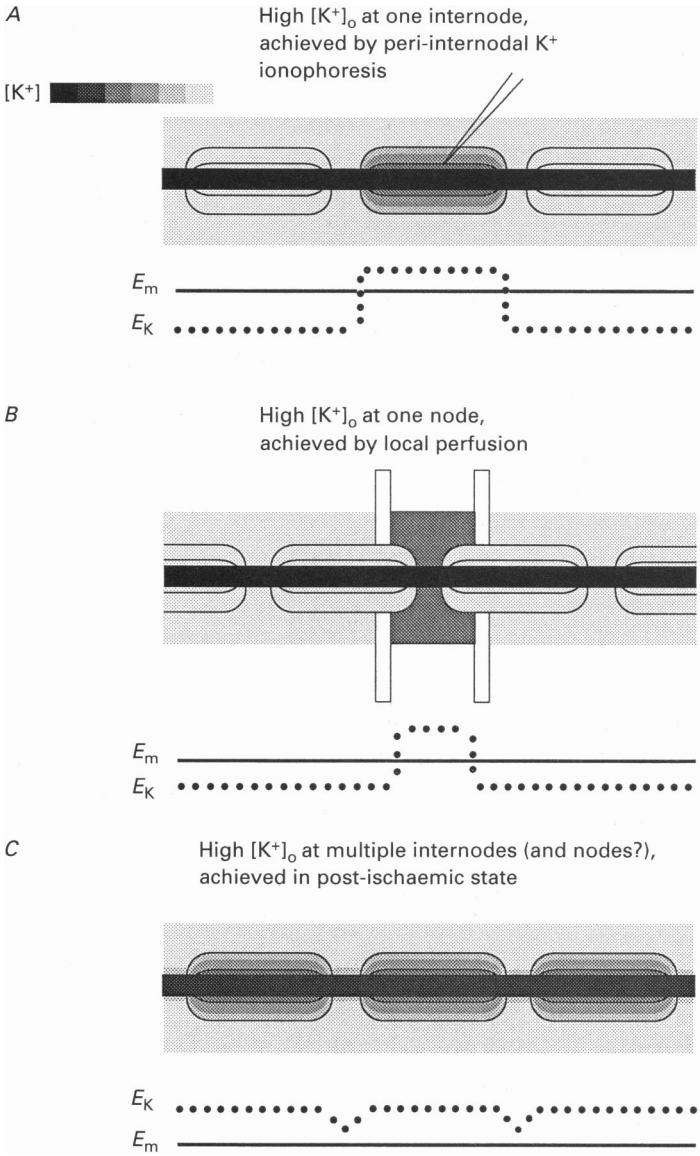

Fig. 12. Hypothesized changes in K^+ distribution (upper) and relationship between the axonal membrane potential E_m and the K^+ equilibrium potential E_K (lower) in three experimental protocols associated with bistable axonal electrical behaviour. Darker shades represent higher $[K^+]$. *A*, elevation of $[K^+]$ in the peri-axonal space of one internode, producing peri-internodal negative potentials (PNPs) in rat (this paper) and lizard motor axons (David *et al.* 1992). *B*, elevation of $[K^+]$ outside a single node, leading to shifts of membrane potential in toad axons (Tasaki, 1959). *C*, elevation of extra-axonal $[K^+]$ and reduction of intra-axonal $[K^+]$ in an *in vivo* human axon in which pump activity has accelerated after a period of ischaemia. This condition is associated with bistable behaviour of axonal threshold in response to externally applied currents (Bostock *et al.* 1991). All diagrams are qualitative, representing the directions, but not the magnitudes, of the hypothesized changes in $[K^+]$, E_K and E_m. The idea that bistable behaviour can occur when E_K becomes more depolarized than E_m is quite similar to the interpretation proposed by Bostock *et al.* (1991).

bring the axonal potential closer to the threshold for action potential initiation, thus favouring the production of ectopic discharges (Fig. 6, see also Bostock *et al.* 1991; Kapoor *et al.* 1992).

The opening of K^+ channels that initiates this regenerative depolarization could occur spontaneously or as a result of applied positive current (Fig. 12*A* and *B*). In the post-ischaemic axon (Fig. 12*C*) the regenerative depolarization might be initiated by a transient reduction of the hyperpolarizing pump current (Bostock *et al.* 1991), or by the opening of axonal inward rectifier channels by the pump-induced hyperpolarization (Baker *et al.* 1987); these channels are permeable to both Na^+ and K^+ (Mayer & Westbrook, 1983; Birch, Kocsis, Di Gregorio, Bhisitkul & Waxman, 1991).

The durations of the reported potential (or threshold) shifts appears to increase with the area of axolemma exposed to the reversed electrochemical K^+ gradient: with only the nodal axolemma exposed to high external $[K^+]$ the membrane potential shifts lasted at most 50 ms (Tasaki, 1959). With the axolemma of one internode exposed to high external $[K^+]$, PNPs lasted hundreds of milliseconds to several seconds (Fig. 4, see also David *et al.* 1992, Kapoor *et al.* 1992). With (presumably) most of the axolemma exposed to elevated external $[K^+]$ in post-ischaemic axons, the threshold shifts measured by Bostock *et al.* (1991) persisted for minutes (assuming that threshold shifts in single axons had the same time course as those measured in the sampled axonal population). Termination of the regenerative K^+ influx could occur by several possible mechanisms: (1) applied hyperpolarization to close delayed rectifier K^+ channels (as in Tasaki, 1959, and David *et al.* 1992); (2) inactivation of delayed rectifier K^+ channels (time course of hundreds of milliseconds to several seconds in axons: Dubois, 1981); (3) depletion of extracellular K^+ (so that E_m becomes equal to or more depolarized than E_K); or (4) activation of K^+ channels in regions of the axon where E_K is more hyperpolarized than E_m.

The duration of the PNP and its prolongation with Rb^+ suggest that K^+ channel inactivation may contribute to PNP termination. The increase in PNP duration (and sometimes amplitude) observed as the interval between PNPs increased (Fig. 4), might have been due to greater buildup of ionophoresed K^+ outside the internodal axolemma, and/or to more time for recovery from K^+ channel inactivation.

Functions of internodal K^+ channels

Chiu & Ritchie (1984) presented calculations and theoretical arguments suggesting that internodal axolemmal K^+ channels contribute to maintenance of the resting potential. If some internodal K^+ channels are indeed open in the resting axon, then one would expect an inward, depolarizing K^+ current across the axolemma of a K^+-loaded internode. If this depolarizing current were not completely offset by K^+ efflux across neighbouring (nodal and internodal) regions of the axolemma which have a normal transmembrane K^+ gradient, then the axolemmal depolarization might itself trigger spontaneous PNPs, such as those observed in K^+-loaded rat internodes (Fig. 4*C*; also Kapoor *et al.* 1992). Spontaneous PNPs were never observed in K^+-loaded lizard internodes, nor were spontaneous action potentials ever observed during the onset of the PNP. These differences between lizard and rat axons suggest that, at potentials near rest, lizard axons have more nodal K^+ channels open, and/or that rat axons have more internodal K^+ channels open. Increased resting activation of

internodal K^+ channels in rat axons might also help explain why the depolarizing after-potential is much smaller in rat than in lizard axons; a high internodal K^+ conductance would reduce the charging of the internodal axolemma by action potential currents.

Chiu & Ritchie (1981) hypothesized that, since mammalian nodal Na^+ channels recover rapidly from inactivation, paranodal K^+ channels might also protect the node from re-excitation by depolarized extra-nodal membranes. Our findings are compatible with this idea, since re-excitation was absent when the electrochemical K^+ gradient across the internodal axolemma was normal, but did occur when this gradient was reversed (Fig. 6*B*).

Data presented here indicate that the internodal K^+ channels in mammalian axons increase their opening in response to action potential activity, raising the possibility that these channels contribute importantly to axonal electrical behaviour during repetitive discharge.

This work was supported by the National Institutes of Health (NS12404) and the National Multiple Sclerosis Society. We thank Dr W. Nonner for reading a preliminary version of this paper and Mr T. Moher and the Olympus Corp. for arranging the confocal microscope demonstration that yielded Fig. 3.

REFERENCES

ANGAUT-PETIT, D., BENOIT, E. & MALLART, A. (1989). Membrane currents in lizard motor nerve terminals and nodes of Ranvier. *Pflügers Archiv* **415**, 81–87.

ARIYASU, R. G., NICHOL, J. A. & ELLISMAN, M. H. (1985). Localization of sodium/potassium adenosine triphosphatase in multiple cell types of the murine nervous system with antibodies raised against the enzyme from kidney. *Journal of Neuroscience* **5**, 2581–2596.

BAKER, M., BOSTOCK, H., GRAFE, P. & MARTIUS, P. (1987). Function and distribution of three types of rectifying channel in rat spinal root myelinated axons. *Journal of Physiology* **383**, 45–67.

BARRETT, E. F. & BARRETT, J. N. (1982). Intracellular recording from vertebrate myelinated axons: mechanism of the depolarizing afterpotential. *Journal of Physiology* **323**, 117–144.

BARRETT, E. F., MORITA, K. & SCAPPATICCI, K. A. (1988). Effects of tetraethylammonium on the depolarizing after-potential and passive properties of lizard myelinated axons. *Journal of Physiology* **402**, 65–78.

BIRCH, B. D., KOCSIS, J. D., DI GREGORIO, F., BHISITKUL, R. B. & WAXMAN, S. G. (1991). A voltage- and time-dependent rectification in rat dorsal spinal root axons. *Journal of Neurophysiology* **66**, 719–728.

BLACK, J. A., KOCSIS, J. D. & WAXMAN, S. G. (1990). Ion channel organization of the myelinated fiber. *Trends in Neurosciences* **13**, 48–54.

BLIGHT, A. R. & SOMEYA, S. (1985). Depolarizing afterpotentials in myelinated axons of mammalian spinal cord. *Neuroscience* **15**, 1–12.

BOSTOCK, H., BAKER, M. & REID, G. (1991). Changes in excitability of human motor axons underlying post-ischaemic fasciculations: evidence for two stable states. *Journal of Physiology* **441**, 537–557.

BOSTOCK, H., SHERRATT, R. M. & SEARS, T. A. (1978). Overcoming conduction failure in demyelinated nerve fibers by prolonging action potentials. *Nature* **274**, 385–387.

BRISMAR, T. (1980). Potential clamp analysis of membrane currents in rat myelinated fibers. *Journal of Physiology* **298**, 171–184.

BRISMAR, T., HILDEBRAND, C. & BERGLUND, S. (1987). Voltage clamp analysis of nodes of Ranvier in regenerated rat sciatic nerve. *Brain Research* **409**, 227–235.

CHIU, S. Y. (1982). Resting potential of a frog myelinated axon: the role of the internode. *Society for Neuroscience Abstracts* **8**, 253.

CHIU, S. Y. (1991). Functions and distribution of voltage-gated sodium and potassium channels in mammalian Schwann cells. *Glia* **4**, 541–558.

CHIU, S. Y. & RITCHIE, J. M. (1980). Potassium channels in nodal and internodal axonal membrane of mammalian myelinated fibres. *Nature* **284**, 170–171.

CHIU, S. Y. & RITCHIE, J. M. (1981). Evidence for the presence of potassium channels in the paranodal region of acutely demyelinated mammalian single nerve fibres. *Journal of Physiology* **313**, 415–437.

CHIU, S. Y. & RITCHIE, J. M. (1982). Evidence for the presence of potassium channels in the internode of frog myelinated nerve fibres. *Journal of Physiology* **322**, 485–501.

CHIU, S. Y. & RITCHIE, J. M. (1984). On the physiological role of internodal potassium channels and the security of conduction in myelinated nerve fibres. *Proceedings of the Royal Society* B **220**, 415–422.

CHIU, S. Y., RITCHIE, J. M., ROGART, R. B. & STAGG, D. (1979). A quantitative description of membrane currents in rabbit myelinated nerve. *Journal of Physiology* **292**, 149–166.

CHIU, S. Y. & SCHWARZ, W. (1987). Sodium and potassium currents in acutely demyelinated internodes of rabbit sciatic nerves. *Journal of Physiology* **391**, 631–649.

CHIU, S. Y., SHRAGER, P. & RITCHIE, J. M. (1985). Loose patch clamp recording of ionic currents in demyelinated frog nerve fibers. *Brain Research* **359**, 338–342.

DAVID, G., BARRETT, J. N. & BARRETT, E. F. (1992). Evidence that action potentials activate an internodal potassium conductance in lizard myelinated axons. *Journal of Physiology* **445**, 277–301.

DUBOIS, J. M. (1981). Evidence for the existence of three types of potassium channels in the frog Ranvier node membrane. *Journal of Physiology* **318**, 297–316.

ENG, D. L., GORDON, T. R., KOCSIS, J. D. & WAXMAN, S. G. (1988). Development of 4-AP and TEA sensitivities in mammalian myelinated nerve fibers. *Journal of Neurophysiology* **60**, 2168–2179.

FRANKENHAEUSER, B. (1959). Steady state inactivation of sodium permeability in myelinated nerve fibres of *Xenopus laevis*. *Journal of Physiology* **148**, 671–676.

FRANKENHAEUSER, B. (1962). Potassium permeability in myelinated nerve fibres of *Xenopus laevis*. *Journal of Physiology* **160**, 54–61.

GASSER, H. S. & GRUNDFEST, H. (1936). Action and excitability in mammalian A fibres. *American Journal of Physiology* **117**, 113–133.

GRISSMER, S. (1986). Properties of potassium and sodium channels in frog internode. *Journal of Physiology* **381**, 119–134.

HILLE, B. (1967). The selective inhibition of delayed potassium currents in nerve by tetraethylammonium ion. *Journal of General Physiology* **50**, 1287–1302.

HILLE, B. (1973). Potassium channels in myelinated nerve; selective permeability to small cations. *Journal of General Physiology* **61**, 669–686.

HILLE, B. (1992). Na and K channels of axons. In *Ionic Channels of Excitable Membranes*, ed. HILLE, B., pp. 59–82. Sinauer Associates, Sunderland, MA, USA.

HOPPE, D., LUX, H. D., SCHACHNER, M. & KETTENMAN, H. (1989). Activation of K^+ currents in cultured Schwann cells is controlled by extracellular pH. *Pflügers Archiv* **415**, 22–28.

JAHROMI, B. H., ROBITAILLE, R. & CHARLTON, M. P. (1992). Transmitter release increases intracellular calcium in perisynaptic Schwann cells in situ. *Neuron* **8**, 1069–1077.

KAPOOR, R., SMITH, K. J., FELTS, P. A. & DAVIES, M. (1992). Cyclical potential changes recorded from rat central and peripheral axons: a mechanism for ectopic impulse generation. *Society for Neuroscience Abstracts* **18**, 74.

KOCSIS, J. D. & WAXMAN, S. G. (1981). Action potential electrogenesis in mammalian central axons. In *Advances in Neurology*, vol. 31, *Demyelinating Diseases, Basic and Clinical Electrophysiology*, ed. WAXMAN, S. G. & RITCHIE, J. M., pp. 299–312. Raven Press, New York.

KONISHI, T. (1990). Dye coupling between mouse Schwann cells. *Brain Research* **508**, 85–92.

MARUHASHI, J. & WRIGHT, E. (1967). Effect of oxygen lack on the single isolated mammalian (rat) nerve fiber. *Journal of Neurophysiology* **30**, 434–452.

MAYER, M. L. & WESTBROOK, G. L. (1983). A voltage-clamp analysis of inward (anomalous) rectification in mouse spinal sensory ganglion neurones. *Journal of Physiology* **340**, 19–45.

MUELLER, P. (1958). Prolonged action potentials from single nodes of Ranvier. *Journal of General Physiology* **42**, 137–162.

PLANT, T. D. (1986). The effect of rubidium ions on components of the potassium conductance in the frog node of Ranvier. *Journal of Physiology* **375**, 81–105.

RITCHIE, J. M. & CHIU, S. Y. (1981). Distribution of sodium and potassium channels in mammalian myelinated nerve. In *Advances in Neurology*, vol. 31, *Demyelinating Diseases, Basic and Clinical Electrophysiology*, ed. WAXMAN, S. G. & RITCHIE, J. M., pp. 329–342. Raven Press, New York.

ROPER, J. & SCHWARZ, J. R. (1989). Heterogeneous distribution of fast and slow potassium channels in myelinated nerve fibres. *Journal of Physiology* **416**, 93–110.

SCHMIDT, H. & STÄMPFLI, R. (1966). Die Wirkung von Tetraäthylammoniumchlorid auf den einzelnen Ranvierschen Schnürring. *Pflügers Archiv* **287**, 311–325.

SMITH, K. J. & SCHAUF, C. L. (1981). Effects of gallamine triethiodide on membrane currents in amphibian and mammalian peripheral nerve. *Journal of Pharmacology and Experimental Therapeutics* **217**, 719–726.

TASAKI, I. (1952). Properties of myelinated fibers in frog sciatic nerve and in spinal cord as examined with micro-electrodes. *Japanese Journal of Physiology* **3**, 73–94.

TASAKI, I. (1959). Demonstration of two stable states of the nerve membrane in potassium-rich media. *Journal of Physiology* **148**, 306–331.

WILSON, G. F. & CHIU, S. Y. (1990). Ion channels in axon and Schwann cell membranes at paranodes of mammalian myelinated fibers studied with patch clamp. *Journal of Neuroscience* **10**, 3263–3274.

WOODBURY, J. W. (1952). Direct membrane resting and action potentials from single myelinated nerve fibers. *Journal of Cellular and Comparative Physiology* **39**, 323–339.